RESEARCH ARTICLE

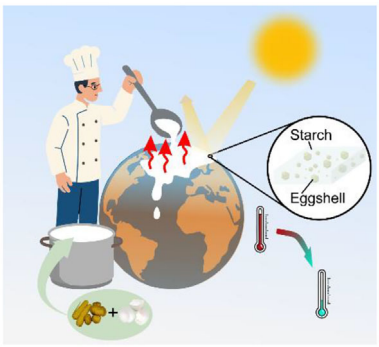

A food-grade cooling composite made from starch and recycled eggshell powder offers a scalable, ultra-low-cost solution for passive daytime radiative cooling. Easily prepared using basic kitchen tools, this material empowers communities, even in areas with limited infrastructure, to stay cooler during worsening summer heat waves. The work highlights a sustainable path to climate resilience using everyday biowaste.

ADVANCED FUNCTIONAL MATERIALS
www.afm-journal.de

Cool Kitchen: Processing Starch and Eggshell Powder into Sustainable Coatings for Passive Daytime Cooling

*Qimeng Song, Evelyn Kubacki, Alexander Berger, and Markus Retsch**

Increasingly frequent and severe heat waves pose a significant threat to human health, intensifying the demand for cooling solutions. Conventional air conditioning offers relief but escalates energy consumption and CO_2 emissions, exacerbating global warming. Here, a passive daytime cooling composite made from kitchen-sourced materials, providing a zero-energy cooling technology accessible to everyone, is introduced. Composed of starch and finely ground eggshell powder, this eco-friendly composite demonstrates an average solar reflectance of 0.91 and thermal emissivity of 0.95. Applied to concrete, it achieves a temperature reduction of approximately 15 °C compared to uncoated concrete under 800 W m^{-2} solar irradiation. With universally accessible ingredients and a simple fabrication process, this cooling composite provides a viable solution for households with limited infrastructure to tackle the growing threat of heat waves.

1. Introduction

Heat-related mortality has evolved into an alarming global crisis, intensifying with soaring temperatures, enduring heatwaves, and the accompanying effects of climate change, posing an ever-more severe threat to vulnerable populations worldwide.[1,2] Recent data highlight the severity of this issue, with over 60 000 heat-related deaths recorded during the record-breaking European summer of 2022 alone.[3] Mitigation strategies, including increasing urban albedo, predictably reducing mortality by ≈1.8% per 0.1 increase, and green infrastructure expansion, have shown promise but remain constrained by cost and feasibility.[4,5] While air conditioning has mitigated some heat-related deaths,[6] its reliance on greenhouse gas-intensive energy sources exacerbates global warming and urban heat islands,[7] further threatening those who cannot afford such systems. These challenges highlight an urgent need for sustainable, cost-effective, and easily deployable solutions that can equitably protect vulnerable communities from intensifying climate-related heat crises.

Aligned with approaches such as increasing surface albedo, passive daytime radiative cooling (PDRC) has recently emerged as a zero-energy strategy, holding great promise to address the growing global energy demand for cooling.[8–10] The core of this sustainable cooling technique lies in tailoring the material to exhibit a minimal solar absorptivity while simultaneously reaching a high emissivity in the mid-infrared (MIR) regime. By effectively radiating excess heat to outer space through the atmospheric transparency window (ATW, 8–13 μm), surpassing the heat absorbed from sunlight, sub-ambient cooling can be theoretically attained. Over the past decade, advanced micro- and nano-fabrication techniques have led to the development of various high-performance PDRC devices, including photonic structured materials,[11,12] composites with embedded micro- and nanoparticles,[13,14] porous polymers and ceramics,[15,16] super white paints,[17,18] and nanofiber membranes.[19–21] Despite their impressive cooling capabilities, these materials concepts often involve sophisticated fabrication processes, advanced manufacturing techniques, or exclusive raw materials, posing challenges for transitioning from laboratory designs to large-scale commercial and affordable products. Therefore, to further expand the global reach of this technique, especially in areas facing poverty and inadequate infrastructure, an urgent need persists for a comprehensive PDRC strategy that employs easily accessible materials and a more straightforward fabrication process.

Starch, a widely distributed plant polysaccharide, is vital in supplying energy for human physiological processes. It is abundantly found in various plant sources globally, such as potato, corn, rice, and cassava.[22] Its molecular structure, rich in —C—O—C— and —C—OH groups, exhibits characteristic MIR absorption bands in the ranges of 1250–1050 cm^{-1} (8–9.5 μm)

Q. Song, E. Kubacki, A. Berger
Department of Chemistry
Physical Chemistry I
University of Bayreuth
Universitätsstraße 30, 95447 Bayreuth, Germany
M. Retsch
Department of Chemistry
Physical Chemistry I
Bavarian Polymer Institute
Bayreuth Center for Colloids and Interfaces
Bayreuther Institut für Makromolekülforschung
and Bavarian Center for Battery Technology (BayBatt)
University of Bayreuth
Universitätsstraße 30, 95447 Bayreuth, Germany
E-mail: markus.retsch@uni-bayreuth.de

The ORCID identification number(s) for the author(s) of this article can be found under https://doi.org/10.1002/adfm.202513897

DOI: 10.1002/adfm.202513897

and 1200–1020 cm^{-1} (8.3–9.8 μm), ensuring an effective heat release through the ATW to the outer space, making it a promising candidate for passive daytime radiative cooling applications. For instance, very recently, Yang et al. reported a porous film for PDRC based on potato starch, achieving promising optical properties.[23] However, their fabrication process involved complex processing steps, and importantly, the study focused solely on potato starch, which has limited water resistance. As a result, additional waterproofing layers were required for outdoor applications. In this work, we systematically evaluated all types of starch, i.e., types A, B, and C, to assess their suitability for passive daytime radiative cooling (PDRC) applications. Furthermore, we developed a simple, sustainable PDRC composite with impressive cooling performance by combining starch with ground white eggshell powder. This solution-processed paint-like composite can be easily prepared with kitchen-level ingredients and tools. It can be applied to various substrates, like bricks, wood, and metal, to reduce solar heating, and it does not require any metallic reflector for its passive cooling performance. The widespread adoption of this technique has the potential to empower households globally to create their own PDRC coating, protecting them from the scorching summer heat and reducing the heat-related mortality burden of forthcoming hotter summers.

2. Results

2.1. Starch: A Natural MIR Emitter

Starch comprises two distinct polysaccharides: amylose, which forms a linear polymer, and amylopectin, which is characterized by branching (**Figure 1A**). The amylose-to-amylopectin ratio varies based on the starch source. Starch can be categorized into A-type, B-type, and C-type based on its crystalline structure, and studies have explored that the origin of the starch-bearing feedstock and crystallinity strongly influence its mechanical and optical properties.[24–26] To comprehensively unveil the potential of starch in the PDRC application across a global spectrum, starch from corn (type A), potato (type B), and tapioca (type C) were investigated in this work. The morphology, size, and crystalline structure of various native starch granules from corn, potato, and tapioca were characterized by scanning electron microscopy (SEM) and X-ray diffraction (XRD), respectively (Figure S1A–D, Supporting information). The observed morphology, size, and crystalline structure characteristics of the various starch granules are consistent with the literature[24,27,28] encompassing starch from diverse geographical regions, demonstrating the universality of starch properties worldwide. To reveal the potential of starch in the application of PDRC, the solar absorption of various native starch powders was first determined with UV–vis spectroscopy. The reflection spectra (Figure S1E, Supporting information) demonstrated a high solar reflectivity for all starch powders within the visible spectral range, which decreased to the ultraviolet (UV) and near-infrared (NIR) spectral range, respectively. The substantial solar scattering and MIR emission expected from the inherent molecular structure render them attractive as a sustainable material for PDRC applications.

When heated in water, starch undergoes a gelatinization process, transforming into a homogenous, viscous, translucent solution that can be readily utilized to create a continuous starch film.[29] Differential scanning calorimetry (DSC) thermograms (Figure 1B) illustrate that all types of starch solution (25 wt%) exhibited gelatinization transitions between 50 and 80 °C. Using doctor blading, we prepared corn, potato, and tapioca starch films with gelatinized starch solutions. The photographs of such starch films prepared on a glass substrate (Figure 1C) demonstrate their semi-transparent appearance. In addition, as the thickness of the corn starch film increased, a significant enhancement in MIR absorption was observed (Figure 1D). Conversely, a slight reduction in solar reflectance was detected with increasing film thickness (Figure S2A, Supporting information), suggesting a minor increase in solar absorption. Furthermore, the solar reflectance and MIR absorption spectra (Figure S2, Supporting information) reveal a consistent influence of film thickness on the optical properties across all three types of starch films, prepared on aluminum (Al) foil as a reflective substrate. We calculated the average reflection in the solar range and average absorption in the ATW range based on an AM 1.5 spectrum[30] and atmospheric transmission.[31] This further clarifies the impact of the starch film thickness on its optical properties (Figure S2C,F,I, Supporting information). As the film thickness increased from 0 μm (plain Al substrate) to ≈35 μm, the emissivity in the ATW range rose significantly from 0.06 to ≈0.95. Conversely, the solar reflectance of all three types of starch showed a slight decrease, from 0.86 (Al substrate) to ≈0.83, indicating a minor increase in solar absorption.

Thin films (≈35 μm) of all three types of starch exhibit negligible absorption in the solar range and outstanding emissivity in the ATW range, making them suitable as emitters for PDRC. To emphasize their thermal emission performance, various starch films were coated onto a highly reflective Ag mirror. All starch film-coated Ag mirrors, with superior broadband optical properties (Figure S3, Supporting information), were demonstrated to have a remarkable passive cooling capacity for both nighttime and daytime (Figure S4, Supporting information). The numerical calculation was conducted based on a widely used radiative model, as detailed in our previous work.[32] To further validate the potential of starch films in PDRC, the cooling performance was evaluated with field testing under a clear sky in Bayreuth, Germany. The starch film-coated Ag mirrors were placed into identical homemade sample holders during the field testing (Figure 1E). Under average solar irradiation of 789 W m^{-2} (11:00–16:00), the average temperature difference relative to the plain mirror was 3.1, 3.6, and 3.8 °C for the corn, potato, and tapioca starch film-coated Ag mirrors, respectively (Figure 1F). We note that even the temperature of the reference mirror, with its minuscule solar absorption and thermal radiation, was observed to be higher than the open-air temperature, which is attributed to an unavoidable greenhouse effect. This greenhouse effect can be rationalized by parasitic solar absorption within the sample holder and the suppression of convection by the LDPE foil.[32] Consequently, all starch film-coated Ag mirrors were observed to have slightly higher temperatures compared to open-air. Without parasitic solar absorption during nighttime, all starch film-coated Ag mirrors exhibited temperatures lower than the open air. Moreover, the temperature of the Ag mirror closely resembled that of the ambient air. The temperature difference to the reference mirror remained almost constant during these conditions (≈3 °C). The remarkable cooling performance of starch films supported

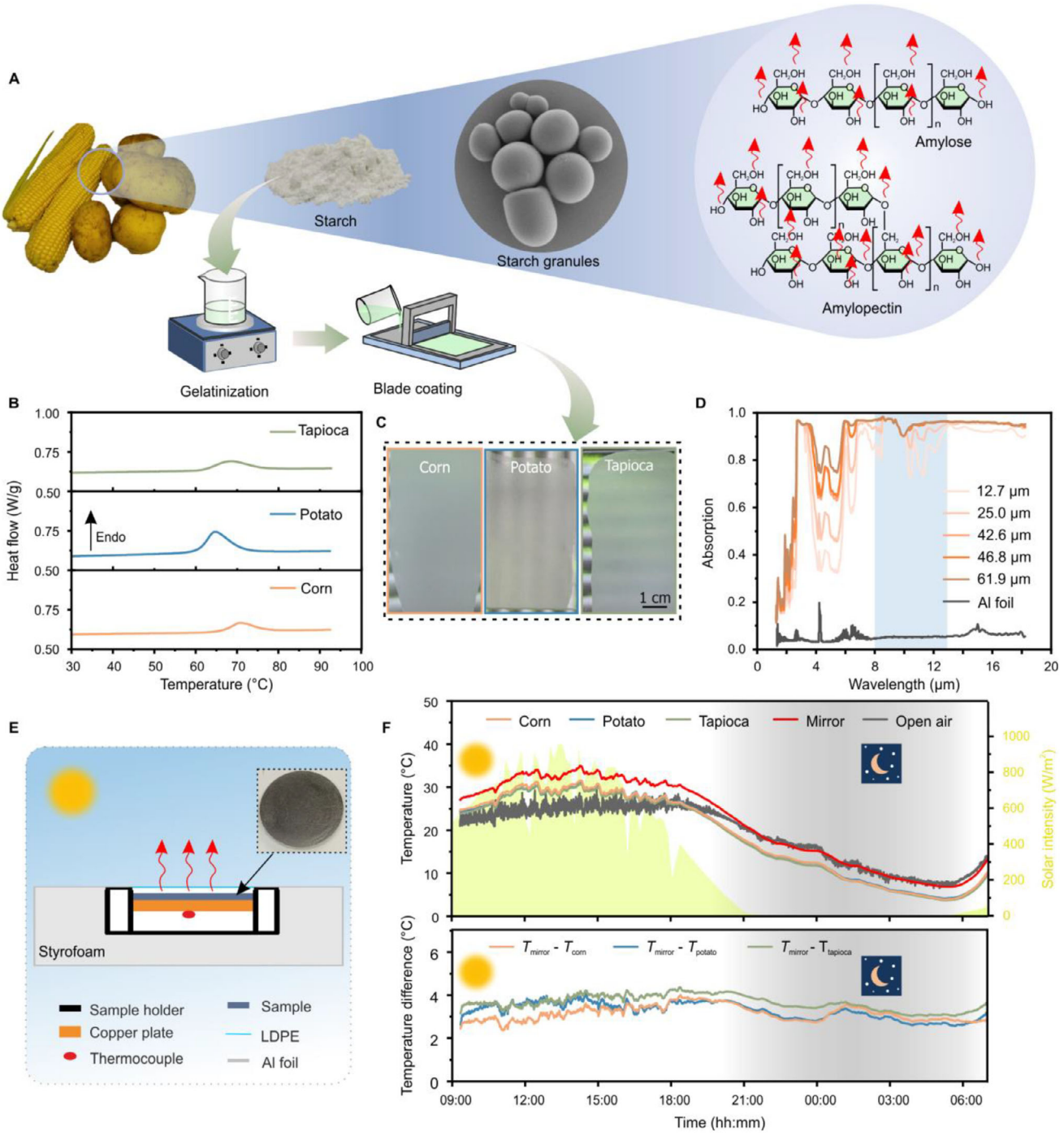

Figure 1. Starch as a natural and universally accessible emitter for thermal radiation. A) Starch multiscale structure and starch film fabrication via blade coating technique. B) DSC thermograms of corn, potato, and tapioca starch. C) Photography of various starch films on a glass substrate, with window blinds in the background. D) MIR absorption of corn starch film on Al foil with various film thicknesses. The atmosphere window (8–13 μm) is indicated with blue shaded area. E) Schematic of the field-testing setup and photography of a starch-coated mirror sample. F) Temperature tracking of various starch film-coated Ag mirrors and temperature difference between uncoated and the starch film-coated Ag mirrors in the field-testing. The outdoor measurement was carried out under a clear sky on June 12th–13th, 2023 in Bayreuth, Germany.

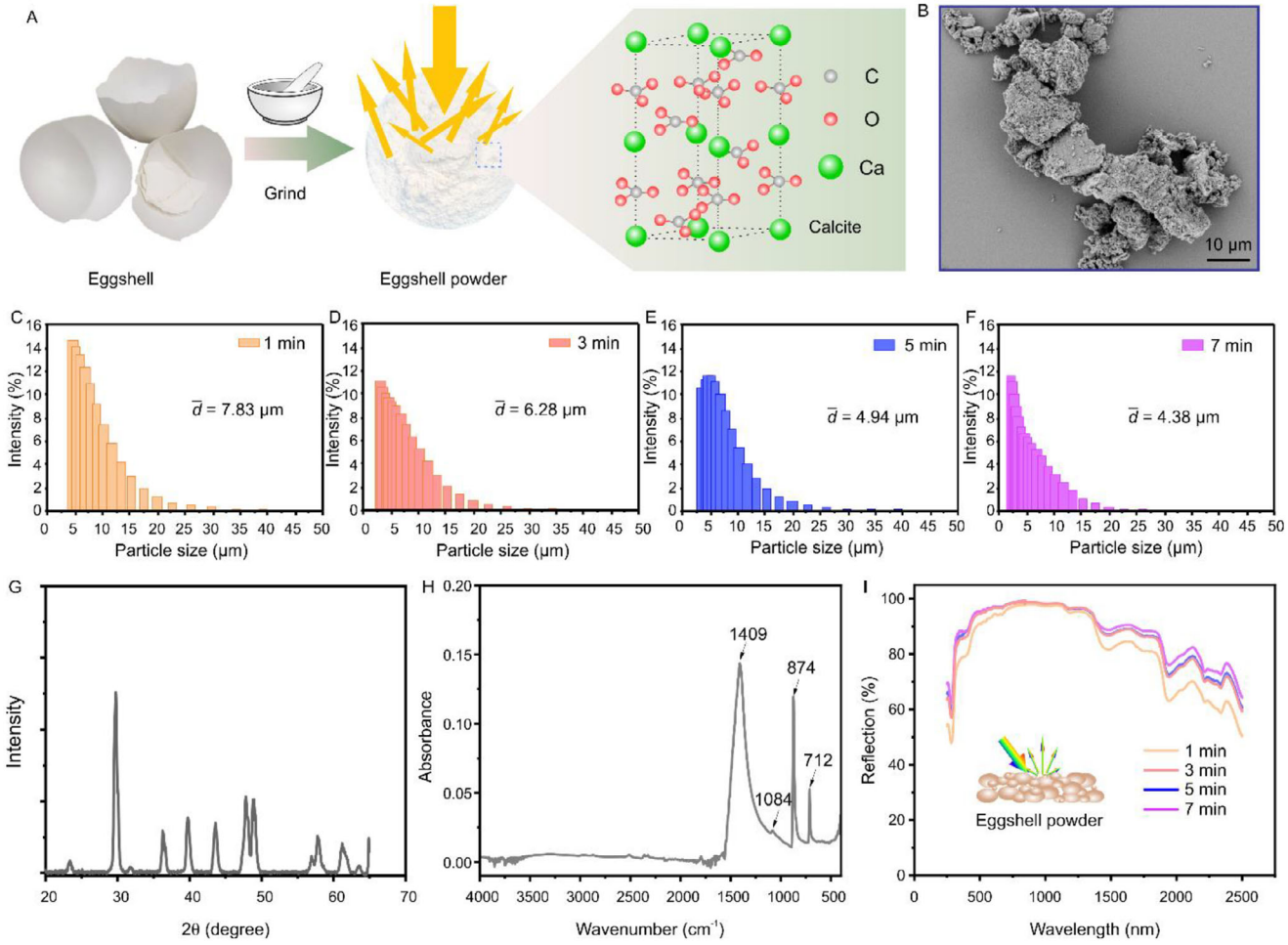

Figure 2. Ground white eggshell powder as a universally accessible and efficient solar light scatterer. A) Preparation of eggshell powder with a traditional mortar and pestle grinding method. B) SEM images of the eggshell powders from native white chicken eggshells. C–F) Number weighted particle size distribution of the eggshell powders prepared with different grinding times, i.e., 1, 3, 5, and 7 min. G) XRD pattern and H) IR absorbance spectrum of the ground eggshell powders. I) UV–vis reflection spectrum of the eggshell powders prepared with different grinding times.

by Ag mirrors underscores their capability as sustainable and universally accessible emitters for PDRC applications.

2.2. Eggshell Powder as an Efficient Solar Light Scatterer

As just outlined above, solar absorption plays a crucial role in daytime passive cooling performance. Even slight solar uptake can significantly counteract the radiative heat release. In addition to employing highly reflective metals like silver or aluminum, nano- and microparticles are extensively used in composite materials to enhance solar scattering through the Mie scattering mechanism.[17,33,34] Calcium carbonate ($CaCO_3$) powder, widely used in coatings and paints, has recently gained attention in PDRC paints and composite materials due to its high solar reflectivity.[17,35] Eggshells are ubiquitous household refuse containing more than 95% calcite ($CaCO_3$) and have been recycled as a sustainable material in various fields, including cementitious materials,[36] coating pigments,[37] heavy metal ions adsorbents,[38] and catalysts.[39] Recently, eggshell powder has also been employed as a solar-scattering filler in PDRC coatings using synthetic polymer matrices such as polymethylpentene (TPX).[40]

Using manual grinding, eggshell waste can be effortlessly converted into eggshell powder (**Figure 2**A,B). The size distribution of the eggshell powders was assessed by static light scattering (SLS) on an aqueous eggshell powder dispersion. We obtained sizes of ≈2–30 μm, with a mean diameter of ≈6 μm. A systematic variation of the grinding time from 1 min to 7 min results in a continuous decrease of the mean particle size from ≈7 to 4 μm (Figure 2C–F). The chemical composition of the eggshell powders derived from native white chicken eggshells was confirmed using XRD and Fourier transform infrared (FTIR) spectroscopy (Figure 2 G, H), in agreement with reported literature.[41,42] The broad particle size distribution and considerable refractive index (n_{CaCO3} = 1.59) result in strong light scattering, as evidenced by the UV–vis reflection spectrum in Figure 2I. The eggshell powder provides strong scattering, particularly between 450 and 1370 nm, rendering it a promising filler component to enhance solar scattering. In addition, the solar reflection was observed to

increase with longer grinding times (Figure 2I). As the grinding duration increased, the average solar reflection of the eggshell powder rose from 91.7% (1 min) to 95.2% (7 min). This enhancement is attributed to stronger light scattering by the finer particles, which more effectively reflect solar radiation.

2.3. Fabrication and Performance of the Starch-Eggshell Cooling Composite

Without a sophisticated fabrication process, a simple paint-like passive cooling composite can be achieved by combining the ground eggshell powder with a gelatinized starch solution (**Figure 3A**). The SEM images in Figure 3B,C show the starch film and the starch-eggshell powder composite, respectively. The solar reflection spectrum (Figure 3D) and calculated average solar reflection (Figure S5, Supporting information) demonstrate that increasing the eggshell powder concentration in the composite and composite thickness enhances solar scattering. With sufficient eggshell powder content (>80 wt%) and layer thickness (>1.2 mm), the starch-eggshell powder composite provides an average solar reflection of 0.91 without any mirror backing, surpassing that of aluminum foil-supported starch films (average solar reflection of 0.83). It also outperforms widely used commercial white paint (Alpina white, Alpina Farben GmbH) of comparable thickness, which contains titanium dioxide and thus possesses considerable UV absorption (Figure 3E). In addition to its excellent optical properties in the solar range, the composite also possesses the necessary optical properties regarding thermal radiation, with an average emissivity of 0.95 within the ATW. The low solar absorption and high thermal radiation culminate in theoretical net cooling powers of 51.7 and 153.1 W m^{-2} for daytime with solar irradiation of 1000 W m^{-2} and nighttime, respectively (Figure S6, Supporting information).

Eggshell powder plays a critical role in controlling the optical performance of the starch-eggshell composite. To investigate the influence of eggshell grinding on the optical properties of the resulting composites, we prepared starch-eggshell powder composites using eggshell powder ground for different durations, i.e., 1, 3, 5, and 7 min. As shown in Figure S7 (Supporting Information), increasing the grinding time led to enhanced solar reflection. The average solar reflection of the composite increased from 86.6% to 93.4% as the grinding time rose from 1 to 7 min, which is attributed to stronger light scattering from the finer particles. These results indicate that sufficient grinding time enables the production of smaller particles, thereby improving the optical performance of the composite. To evaluate the reproducibility of the fabricated starch-eggshell cooling composite, we asked three individuals to independently prepare eggshell powders while using no recommended grinding time. As shown in Figure S8 (Supporting Information), the resulting particle size distributions are quite similar, with sizes ranging from 2 to 35 µm. Remarkably, the average particle size turned out to be 4–6 µm in all cases. All samples show an average solar reflectance of ≈92%, indicating that the fabrication approach is reproducible and robust against small variations in particle size. Furthermore, three independent grinding repetitions conducted with the same individual also showed consistently high solar reflectance (Figure S9, Supporting Information), confirming the reproducibility of the process despite small differences in particle size.

The starch and eggshell powder-derived PDRC composite is eco-friendly, extremely low-cost, and can be readily prepared with kitchen-level tools. Significantly, its paint-like characteristics enable versatile coating possibilities onto a range of materials, e.g., concrete (Figure 3F, left), wood (Figure 3F, middle), and Al foil (Figure 3F, right), effectively reducing their solar absorption. It should be noted that for thicker starch-eggshell composite coatings, cracks tend to form during drying due to shrinkage stresses. Therefore, multiple successive coatings are required to achieve a fully covered film. Despite the presence of cracks, the starch-eggshell composite adheres strongly to the substrate, as demonstrated by the tape adhesion test (Figure S10, Supporting information). To emphasize the solar reflection capabilities of the composite, we coated the composite on a graphite-covered aluminum foil. Subsequently, the composite-coated and pristine graphite-Al foil was exposed to AM 1.5 solar light. As illustrated in Figure 3G, after one hour of solar irradiation, the uncoated graphite-Al foil reached 48.6 °C. In contrast, the composite-coated graphite-Al foil maintained a significantly lower temperature of 33.8 °C, highlighting the composite's remarkable solar reflection properties without any metallic backing layer. To evaluate the cooling performance of starch and eggshell powder-derived PDRC composites and Al foil supported-starch cooling films, three identical concrete slabs with different surface modifications were placed under the clear sky during the daytime on August 11th, 2023. Thereby, one concrete slab was coated with starch-eggshell composite (C3), another was covered with Al foil supported-starch film (C2), and the third one was left untreated (C1). As the IR images infer in Figure 3h, the coated concretes (C3 and C2) remained significantly cooler than the untreated concrete (C1) under direct sunlight with an intensity of about 800 W m^{-2}. We attribute this to the substantial solar scattering and heat-releasing capabilities of the starch-modified slabs. The recorded temperatures (Figure 3I,J) reveal that the average temperature difference between C1 and C2, C1 and C3 was 13.9 and 14.9 °C, respectively, from 11:00 to 16:00. The significantly lower temperatures attained with the starch-eggshell powder composite and aluminum foil-backed starch film underscore the efficacy of this sustainable and universally accessible PDRC coating.

We determined the water stability of the three starch films by immersing them in water for varying durations. All three starch films exhibited a rapid initial water uptake within the first few minutes (Figure S11A, Supporting information). The swelling ratio ($(m_{swollen} - m_{dry}) / m_{dry}$) reached its maximum within a minute of immersion, with values of 338%, 563%, and 433% for corn, potato, and tapioca starch films, respectively. Corn starch film retained its mass upon further immersion, contrasting with potato and tapioca starch films, which experienced gradual mass loss attributed to substrate detachment. This enhanced stability is attributed to the higher amylose content in corn starch, which promotes a denser, more water-resistant film structure.[43] Moreover, eggshell powder has been reported to improve the mechanical properties of the starch film by enhancing hydrogen bonding.[44] The water stability of the corn starch-eggshell powder cooling composite was validated through a 24-h immersion test in water. The composite was observed to retain its structural integrity

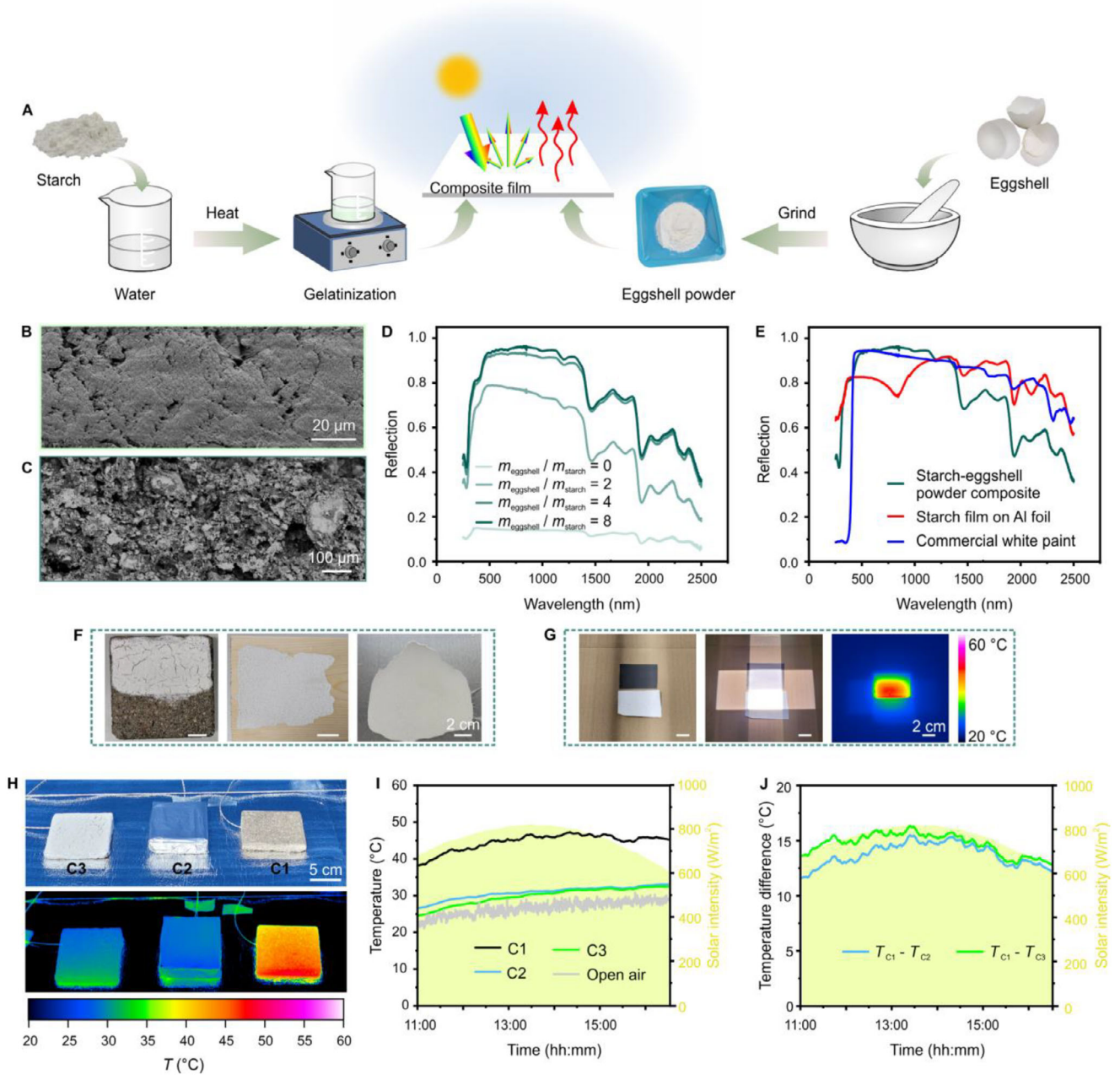

Figure 3. Performance evaluation of the starch-eggshell powder composite for passive cooling applications. A) Schematic of the PDRC starch-eggshell powder composite fabrication. B,C) SEM image of (B) plain starch film and (C) starch-eggshell powder composite, with a mass ratio ($m_{eggshell}$ / m_{starch}) of 8:1. D) Solar reflection spectrum of starch-eggshell powder composite with various mass ratio. E) Solar reflection spectrum of starch-eggshell powder composite ($m_{eggshell}$ / m_{starch} = 8:1), Al foil-backed starch film and commercial white paint (Alpina white). F) Photography of starch-eggshell powder composite-coated concrete slab (left), wood (middle), and Al foil (right). G) Photography and IR image of a starch-eggshell powder composite coated and pristine graphite-covered Al foil under the AM 1.5 solar illumination. H) Photography and IR image of an uncoated concrete slab (C1), a concrete slab covered with a starch-film coated Al foil (C2), and a concrete slab covered with a starch-eggshell powder composite- (C3) under direct sunlight. I) Temperature tracking of the concrete slabs. J) Temperature difference between the coated and uncoated concrete slabs. The measurement was performed under a clear sky on August 11th, 2023 in Bayreuth, Germany.

and experienced a 1.43-fold increase in mass due to swelling (Figure S11B,C, Supporting information). The swollen state resulted in a decline in solar reflection, from 0.91 in the dry to 0.79 in the wet state. Interestingly, upon redrying the composite, the initial mass and reflection properties were fully restored (Figure S11B,C, Supporting information), implying its structural stability for humidity uptake and release upon outdoor operation. Furthermore, evaporative cooling induced by the evaporation of water stored in the swollen composite contributes as a latent heat sink to the overall passive cooling capacity of the composite.[45]

To further demonstrate the outdoor durability of the corn starch-eggshell powder composite, we conducted an accelerated weathering test using a Q-SUN XE-3 test chamber (Q-Lab Corporation, Westlake, OH, USA). The samples were exposed to a UV irradiance of 60 W m^{-2}, a temperature of 38 °C, and 50% relative humidity for 7 days. Under these conditions, the 7-day test corresponds to ≈35 days of natural weathering in central Europe, based on a validated fivefold acceleration factor reported in the literature.[46] As shown in Figure S12 (Supporting Information), no visible degradation was observed on the composite-coated aluminum plates. This visual stability is further supported by optical characterization, as the solar reflectance spectra before and after weathering exhibit no obvious changes, indicating good resistance to UV-induced aging and excellent outdoor stability. In addition, given the anti-fouling properties of $CaCO_3$ particles[47,48] and its high loading ratio (89 wt%) in our composite material, we do not expect a fast-cooling deterioration due to mold formation. No visible signs of mold formation or reduction in solar reflectance were observed in the corn starch-eggshell composite stored indoors for over 1.5 years under ambient conditions (Figure S13, Supporting Information), confirming its long-term stability against microbial degradation in dry environments. We also tested the coating for its resilience to rain. Here, the coating can gradually wash off, posing no environmental concern due to its biodegradable components. Under arid conditions, the eggshell/starch composite can be expected to last for multiple months.

Paint-like PDRC materials with notable optical properties, such as solar reflectance values up to 0.97, have been reported in the literature, as summarized in Table S1 (Supporting Information). These materials demonstrate outstanding cooling performance but strongly rely on synthetic components, organic solvents, and complex fabrication processes, which limit their usability to small areas or few expert users; they may incur substantial costs or impose environmental concerns due to the presence of nondegradable components such as fluorinated hydrocarbons. In comparison, although the solar reflectance of our starch-eggshell composite (0.91) is slightly lower and requires a higher thickness (>1.2 mm) than the state-of-the-art PDC coatings, our approach offers a key advantage: it allows anyone to prepare effective cooling materials at home using common, biodegradable ingredients. Since the main component of the composite is recycled eggshell biowaste (over 80 wt%), the material cost remains extremely low. This do-it-yourself strategy bypasses the need for industrial manufacturing or commercial products, making passive cooling accessible to communities with limited infrastructure.

3. Conclusion

In this study, we explored a sustainable PDRC composite by integrating starch and ground white eggshell powders. This solution-processed and paint-like composite can easily be applied to various substrates, enhancing solar scattering. With satisfactory optical properties, including an average solar reflection of 0.91 and an emissivity of 0.95, the cooling composite enables a coated concrete slab to be ≈15 °C cooler than its uncoated counterpart even under harsh sunlight. Based on the universally available starch and kitchen-level fabrication process, the proposed cooling composite will empower everyone, even in regions with poor infrastructure, to counteract the increasing frequency and intensity of heat waves, thereby alleviating the rising heat-related mortality.

4. Experimental Section

Fabrication of Starch Films: Various starch solutions with a concentration of 5 wt% were prepared in glassware equipped with a string bar. The starch solutions were then placed in an oil bath for 1 h with continuous stirring for gelatinization. The gelatinization temperature is 90 and 85 °C for corn, potato, and tapioca starch, respectively. The resulting gelatinized starch solution was then cooled to room temperature for further processing.

For the starch film with various thicknesses, the gelatinized starch solution was coated on an Al foil with various thicknesses via doctor blading. The starch films were then dried at ambient temperature overnight. For the starch film-coated Ag mirror samples, the blade coating was done directly on an Ag mirror.

Fabrication of Starch-Eggshell Composite: Eggshells from regular white chicken eggs were rinsed with water, manually peeled to remove the inner membrane, and air-dried at ambient temperature. The dried shells were then manually ground using a traditional ceramic mortar and pestle in a continuous process, applying firm, circular pressing motions for ≈10 min until a fine and uniform powder was obtained. The resulting eggshell powders were then mixed with the gelatinized starch solution without further treatment.

Differential Scanning Calorimetry (DSC): Measurements were carried out using a Discovery DSC 2500 (TA Instruments, USA). Starch solutions with concentrations of 25 and 5 wt% were prepared for three different starches by dispersing the starch granules in Milli-Q water. The starch solutions were then placed at ambient temperature for 4 h for starch swelling. About 25 mg of the starch solution was placed into a DSC pan, which was then sealed to prevent water evaporation. The DCS pan was heated between 15 and 95 °C at a rate of 10 K min^{-1} and in a nitrogen atmosphere. An identical empty DSC pan was used as the reference. The first heating cycle was used for the evaluation.

X-Ray Diffraction (XRD): Powder XRD was done using a Bragg–Brentano geometry on a PANalytical Empyrean diffractometer (Malvern PANalytical BV, the Netherlands). The diffractometer is equipped with a PIXcel1D-Medipix3 detector in spinning mode using Cu K-α radiation (λ = 1.5406 Å).

Scanning Electron Microscopy (SEM): SEM images of various starch granules were obtained with a Zeiss Ultra plus (Carl Zeiss AG, Germany). An operating voltage of 3 kV and a working distance of 6.5 mm were applied during the measurements.

Optical Characterization: The optical properties in the UV–vis-NIR regime were determined by using a UV−vis spectrometer (Cary 5000, Agilent Technologies) equipped with an integrating sphere accessory (Labspheres) at a fixed incident angle of 8°. A reference point was established using a Spectralon diffuse reflectance standard (Labspheres). The optical properties in the MIR regime were obtained with an FTIR spectroscope (Vertex 70, Bruker) coupled with a gold-coated integrating sphere accessory (A562, Bruker). A gold mirror served as the reference. Absorption/emission was calculated by subtracting reflection from 1 since the presence of the Al layer or Ag layer rendered transmission negligible.

Field Testing: Outdoor measurements of the starch film-coated Ag mirrors were carried out under a clear sky (June 12th–13th, 2023, University of Bayreuth, Bayreuth, Germany) on the roof of a three-floor building. Identical homemade sample holders were used for all test samples. These holders were insulated with Styrofoam and wrapped in Mylar aluminum foil for thermal protection. LDPE foil, with a thickness of ≈15 µm, was utilized to mitigate convective heat transfer. Pt-100 temperature sensors were employed to ascertain the sample temperatures, and these readings were captured every 5 s using a digital multimeter (DAQ6510, Tektronix, Germany). Solar irradiance data was sourced from the weather station at

the University Bayreuth (Ecological-Botanical Garden), situated ≈400 m away from the rooftop measurement location.

Numerical Simulation: The average solar reflectance of the samples was calculated with the equation:

$$\bar{R}_{\text{Solar}} = \frac{\int_{0\mu m}^{2.5\mu m} I_{\text{solar}}(\lambda) \cdot R_{\text{solar}}(\lambda)\, d\lambda}{\int_{0\mu m}^{2.5\mu m} I_{\text{solar}}(\lambda)\, d\lambda} \quad (1)$$

where $I_{\text{solar}}(\lambda)$ is the ASTM G173 Global solar intensity spectrum, λ is the wavelength, and $R_{\text{solar}}(\lambda)$ is the surface spectral reflectance.

Average absorptance/emittance ($\bar{\varepsilon}$) of the samples in the ATW range was calculated by:

$$\bar{\varepsilon} = \frac{\int_{8\mu m}^{13\mu m} I_{BB}(T, \lambda) \cdot \varepsilon(T, \lambda)\, d\lambda}{\int_{8\mu m}^{13\mu m} I_{BB}(T, \lambda)\, d\lambda} \quad (2)$$

where $I_{BB}(T, \lambda)$ is the spectral emittance of a blackbody at temperature T and $\varepsilon(T, \lambda)$ is the surface spectral emittance. $T = 300$ K is applied to all $\bar{\varepsilon}$ calculations.

Net cooling power calculation of the samples was based on the energy balance: $P_{\text{cool}} = P_{\text{mat}} - P_{\text{sun}} - P_{\text{atm}} - P_{\text{nonrad}}$, Where P_{mat} is the thermal irradiation power of the emitter, P_{sun} is the material's absorbed solar power, P_{atm} is the material's absorbed power from the atmosphere, and P_{nonrad} is the conduction and convection-induced heat exchange. P_{nonrad} can be calculated by $P_{\text{nonrad}} = h_c * (T_{\text{atm}} - T_{\text{mat}})$, where h_c is the nonradiative heat transfer coefficient. For simplicity, the emissivity of all cooling samples was assumed to be directional-independent.

Supporting Information

Supporting Information is available from the Wiley Online Library or from the author.

Acknowledgements

The authors thank Stefan Rettinger and the mechanical workshop (University Bayreuth) for technical support. The authors gratefully thank Prof. Christoph Thomas for kindly providing the solar radiance data, Prof. Breu providing access to the particle size characterization, and Prof. Agarwal and Dr. Wagner providing access to the accelerated weather testing. The authors thank M.Sc. Felix Uhlig for the help with the SLS measurements and M.Sc. Flora Lebeda for COMSOL simulations. The authors thank M.Sc. Viktoria Veitengruber, M.Sc. Simon Freund, M.Sc. Sudeshna Sahoo for their support with the reproducibility experiments. The Keylab "Electron Microscopy" (University Bayreuth) is thanked for SEM measurements. A.B. thanks the Elite Network of Bavaria (ENB). The authors acknowledge financial support from the European Research Council (ERC) under the European Union's Horizon 2020 research and innovation program (grant agreement no. 101082087) and from the German Research Foundation within the IRTG Optexc (grant no. 464648186)

Open access funding enabled and organized by Projekt DEAL.

Conflict of Interest

The authors declare no conflict of interest.

Data Availability Statement

The data that support the findings of this study are available from corresponding author upon reasonable request.

Keywords

biogenic materials, composites, eggshell waste upcycling, radiative cooling, thermal management

Received: June 2, 2025
Revised: July 16, 2025
Published online:

[1] S. Luthi, C. Fairless, E. M. Fischer, N. Scovronick, A. Ben, M. Coelho, Y. L. Guo, Y. Guo, Y. Honda, V. Huber, J. Kysely, E. Lavigne, D. Roye, N. Ryti, S. Silva, A. Urban, A. Gasparrini, D. N. Bresch, A. M. Vicedo-Cabrera, *Nat. Commun.* **2023**, *14*, 4894.
[2] H. Chen, L. Zhao, L. Cheng, Y. Zhang, H. Wang, K. Gu, J. Bao, J. Yang, Z. Liu, J. Huang, Y. Chen, X. Gao, Y. Xu, C. Wang, W. Cai, P. Gong, Y. Luo, W. Liang, C. Huang, *Lancet Reg. Health West Pac.* **2022**, *28*, 100582.
[3] J. Ballester, M. Quijal-Zamorano, R. F. Mendez Turrubiates, F. Pegenaute, F. R. Herrmann, J. M. Robine, X. Basagana, C. Tonne, J. M. Anto, H. Achebak, *Nat. Med.* **2023**, *29*, 1857.
[4] M. Santamouris, F. Fiorito, *Sol. Energy* **2021**, *216*, 493.
[5] A. Tiwari, P. Kumar, G. Kalaiarasan, T. B. Ottosen, *Environ. Pollut.* **2021**, *274*, 115898.
[6] M. S. O'Neill, A. Zanobetti, J. Schwartz, *J. Urban Health* **2005**, *82*, 191.
[7] J. Woods, N. James, E. Kozubal, E. Bonnema, K. Brief, L. Voeller, J. Rivest, *Joule* **2022**, *6*, 726.
[8] M. Chen, D. Pang, X. Chen, H. Yan, Y. Yang, *EcoMat* **2021**, *4*, 12153.
[9] X. Yin, R. Yang, G. Tan, S. Fan, *Science* **2020**, *370*, 786.
[10] S. Wu, Y. Cao, Y. Li, W. Sun, *Adv. Opt. Mater.* **2022**, *11*, 2202163.
[11] A. P. Raman, M. A. Anoma, L. Zhu, E. Rephaeli, S. Fan, *Nature* **2014**, *515*, 540.
[12] Y. Jin, Y. Jeong, K. Yu, *Adv. Funct. Mater.* **2022**, *33*, 2207940.
[13] Y. Zhai, Y. Ma, S. N. David, D. Zhao, R. Lou, G. Tan, R. Yang, X. Yin, *Science* **2017**, *355*, 1062.
[14] X. Zhao, T. Li, H. Xie, H. Liu, L. Wang, Y. Qu, S. C. Li, S. Liu, A. H. Brozena, Z. Yu, J. Srebric, L. Hu, *Science* **2023**, *382*, 684.
[15] J. Mandal, Y. Fu, A. C. Overvig, M. Jia, K. Sun, N. N. Shi, H. Zhou, X. Xiao, N. Yu, Y. Yang, *Science* **2018**, *362*, 315.
[16] K. Lin, S. Chen, Y. Zeng, T. C. Ho, Y. Zhu, X. Wang, F. Liu, B. Huang, C. Y. Chao, Z. Wang, C. Y. Tso, *Science* **2023**, *382*, 691.
[17] X. Li, J. Peoples, Z. Huang, Z. Zhao, J. Qiu, X. Ruan, *Cell Rep. Phys. Sci.* **2020**, *1*, 100221.
[18] X. Li, J. Peoples, P. Yao, X. Ruan, *ACS Appl. Mater. Interfaces* **2021**, *13*, 21733.
[19] X. Wang, X. H. Liu, Z. Y. Li, H. W. Zhang, Z. W. Yang, H. Zhou, T. X. Fan, *Adv. Funct. Mater.* **2020**, *30*, 1907562.
[20] S. Zeng, S. Pian, M. Su, Z. Wang, M. Wu, X. Liu, M. Chen, Y. Xiang, J. Wu, M. Zhang, Q. Cen, Y. Tang, X. Zhou, Z. Huang, R. Wang, A. Tunuhe, X. Sun, Z. Xia, M. Tian, M. Chen, X. Ma, L. Yang, J. Zhou, H. Zhou, Q. Yang, X. Li, Y. Ma, G. Tao, *Science* **2021**, *373*, 692.
[21] H. Zhong, Y. Li, P. Zhang, S. Gao, B. Liu, Y. Wang, T. Meng, Y. Zhou, H. Hou, C. Xue, Y. Zhao, Z. Wang, *ACS Nano* **2021**, *15*, 10076.
[22] L. Copeland, J. Blazek, H. Salman, M. C. Tang, *Food Hydrocolloids* **2009**, *23*, 1527.
[23] Y. Liu, A. Caratenuto, X. Zhang, Y. Mu, Y. Jeyar, M. Antezza, Y. Zheng, *J. Mater. Chem. A.* **2025**, *13*, 10792.
[24] L. A. Muñoz, F. Pedreschi, A. Leiva, J. M. Aguilera, *J. Food Eng.* **2015**, *152*, 65.
[25] S. Wang, C. Chao, F. Xiang, X. Zhang, S. Wang, L. Copeland, *Sci. Rep.* **2018**, *8*, 3011.
[26] R. Thakur, P. Pristijono, C. J. Scarlett, M. Bowyer, S. P. Singh, Q. V. Vuong, *Int. J. Biol. Macromol.* **2019**, *132*, 1079.

[27] V. Singh, S. Z. Ali, R. Somashekar, P. S. Mukherjee, *Int. J. Food Prop.* **2006**, *9*, 845.
[28] K. Dome, E. Podgorbunskikh, A. Bychkov, O. Lomovsky, *Polymers (Basel)* **2020**, *12*, 641.
[29] W. S. Ratnayake, D. S. Jackson, *Adv. Food Nutr. Res.* **2009**, *55*, 221.
[30] Solar Spectral Irradiance: Air Mass 1.5. available at: http://rredc.nrel.gov/solar/spectra/am1.5, (accessed: May, 2024).
[31] Spectral atmospheric transmittance. available at: https://www.gemini.edu/observing/telescopes-and-sites/sites#Transmission, (accessed: May, 2024).
[32] K. Herrmann, T. Lauster, Q. Song, M. Retsch, *Adv. Energy Sustainability Res.* **2021**, *3*, 2100166.
[33] R. A. Yalçın, E. Blandre, K. Joulain, J. Drévillon, *ACS Photonics* **2020**, *7*, 1312.
[34] W. Huang, Y. Chen, Y. Luo, J. Mandal, W. Li, M. Chen, C. C. Tsai, Z. Shan, N. Yu, Y. Yang, *Adv. Funct. Mater.* **2021**, *31*, 2010334.
[35] Y. Tao, Z. Mao, Z. Yang, J. Zhang, *J. Vinyl Add. Tech.* **2020**, *27*, 275.
[36] D. Yang, J. Zhao, W. Ahmad, M. Nasir Amin, F. Aslam, K. Khan, A. Ahmad, *Constr. Build. Mater.* **2022**, *344*, 128143.
[37] S. Yoo, J. S. Hsieh, P. Zou, J. Kokoszka, *Bioresour. Technol.* **2009**, *100*, 6416.
[38] M. Balaz, J. Ficeriova, J. Briancin, *Chemosphere* **2016**, *146*, 458.
[39] H. Liu, Y. Liu, L. Tang, J. Wang, J. Yu, H. Zhang, M. Yu, J. Zou, Q. Xie, *Sci. Total Environ.* **2020**, *745*, 141095.
[40] S. Wu, R. Jian, L. Zhou, S. Tian, T. Luo, S. Cui, B. Zhao, G. Xiong, *ACS Appl. Mater. Interfaces* **2023**, *15*, 44820.
[41] D. Cree, A. Rutter, *ACS Sustainable Chem. Eng.* **2015**, *3*, 941.
[42] J. D. Rodriguez-Blanco, S. Shaw, L. G. Benning, *Nanoscale* **2011**, *3*, 265.
[43] A. Cano, A. Jimenez, M. Chafer, C. Gonzalez, A. Chiralt, *Carbohydr. Polym.* **2014**, *111*, 543.
[44] H. Xu, J. Li, D. J. McClements, H. Cheng, J. Long, X. Peng, Z. Xu, M. Meng, Y. Zou, G. Chen, Z. Jin, L. Chen, *Int. J. Biol. Macromol.* **2023**, *253*, 127165.
[45] L. Xu, D.-W. Sun, Y. Tian, T. Fan, Z. Zhu, *Chem. Eng. J. (Lausanne)* **2023**, *457*, 141231.
[46] N. Meides, A. Mauel, T. Menzel, V. Altstädt, H. Ruckdäschel, J. Senker, P. Strohriegl, *Microplast. Nanoplast.* **2022**, *2*, 23.
[47] A. K. Nair, A. M. Isloor, R. Kumar, A. F. Ismail, *Desalination* **2013**, *322*, 69.
[48] T. Motlhalamme, H. Mohamed, A. G. Kaningini, G. K. More, F. T. Thema, K. C. Mohale, M. Maaza, *Plant Nano Biology* **2023**, *6*, 100050.